



# A colorimetric and fluorescence turn-on probe for the detection of palladium in aqueous solution and its application *in vitro* and *in vivo*

Qi Sun,<sup>a, #</sup> Yuan Qiu,<sup>a, #</sup> Jun Chen,<sup>a</sup> Feng-Shou Wu,<sup>a</sup> Xiao-Gang Luo<sup>a, d</sup> Yan-Rong Guo,<sup>c</sup> Xin-Ya Han<sup>c, \*</sup> and Da-Wei Wang<sup>b, \*</sup>

<sup>a</sup> Key Laboratory for Green Chemical Process of Ministry of Education, School of Chemistry and Environmental Engineering, Wuhan Institute of Technology, Wuhan 430205, China.

<sup>b</sup> State Key Laboratory of Elemento-Organic Chemistry, and Department of Chemical Biology, National Pesticide Engineering Research Center, Collaborative Innovation Center of Chemical Science and Engineering, College of Chemistry, Nankai University, Tianjin 300071, P. R. China.

<sup>c</sup> School of Chemistry and Chemical Engineering, Anhui University of Technology, Maanshan 243002, China.

<sup>d</sup> School of Materials Science and Engineering, Zhengzhou University, No.100 Science Avenue, Zhengzhou City, 450001, Henan Province, PR China

<sup>#</sup> These authors contributed equally to this work.

Corresponding authors:

E-mail addresses: xinyahan@ahut.edu.cn (X. Y. Han); wangdw@nankai.edu.

**ABSTRACT:** Palladium has attracted a growing number of attention due to its widely application and environmental toxicity. Consequently, a novel colorimetric and fluorescent turn-on probe (**NT-Pd**) was designed for sensing of palladium. This probe was capable of detecting palladium in aqueous solution (DMSO was less than 1 %, v/v). Under this mild condition, **NT-Pd** displayed high selectivity and sensitivity for sensing of palladium in both colorimetric and fluorescent strategy, such as low detection limit (5.30 nM) and rapid response time (within 10 min). In addition,

**NT-Pd** was successfully applied for imaging of exogenous palladium in living cells and zebrafishes with good biocompatibility and low toxicity, indicating this probe has satisfactory application potential to track palladium in the complicated biological system.

**Keywords:** Fluorescence probe; Palladium; Bioimaging; Zebrafish

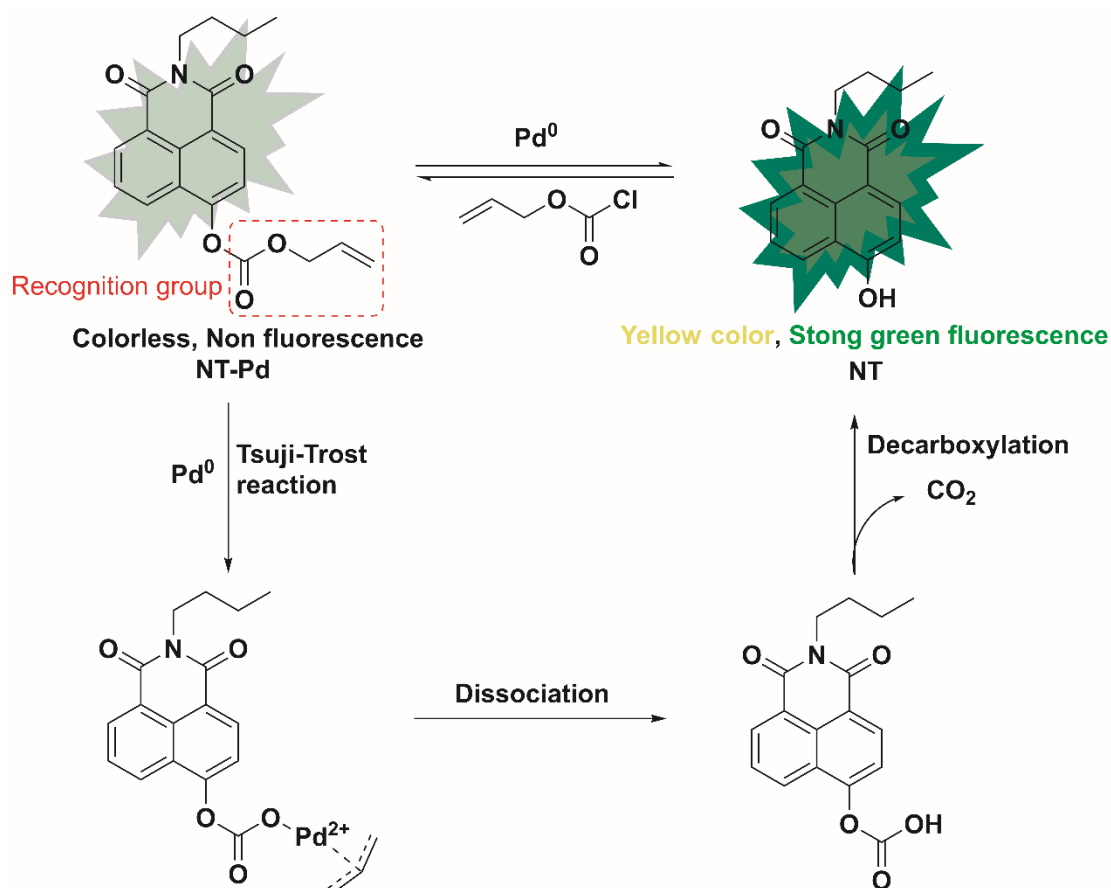
## Introduction

Palladium (Pd), a rare transition metal, was first discovered by William Hyde Wollaston in 1803 [1-2]. To date, it is widely applied in chemistry, biology and environmental science owing to its special physical and chemical properties [3-4]. For instance, palladium-containing catalyst including Pd(PPh<sub>3</sub>)<sub>4</sub>, PdCl<sub>2</sub>, Pd(CH<sub>3</sub>COO)<sub>2</sub>, (CH<sub>3</sub>CN)<sub>2</sub>PdCl<sub>2</sub>, etc. is widely used due to its excellent catalytic ability which lead to a significant effect on the progress of organic chemistry [5-8]. In addition, various palladium-containing reagent has been reported as potential drugs for cancer cells, which exhibit high anti-cancer activity [9]. Furthermore, as we know, palladium is also used for jewelry, electric equipment, dental restorations and so on [11-12]. Although palladium has extensive practical applications in various fields, it may lead to palladium accumulation in the environment [1]. This high concentration of palladium would cause potential toxicity to human health because palladium is capable of binding closely to biomolecules including thiol-containing protein, amino acids, DNA, RNA, etc. [13-15]. Consequently, to protect people's health, the European Agency for the Evaluation of Medicinal Products (EMA) reports the concentration limits of palladium which the palladium-containing drugs is 5-10 ppm and the recommended daily meal intake is less than 1.5-15 μM [16-17]. Hence, efficient strategy for simple and rapid detection of palladium are very urgent and important in biological systems and environment.

So far, several traditional testing methods, such as atomic absorption spectrometry (AAS), inductively coupled plasma mass spectrometry (ICP-MS), high performance liquid chromatography (HPLC) and X-ray fluorescence (XRF), have been

successfully used for palladium detection [18-21]. Although these strategies are prominent sensitive to palladium, it still has some shortcomings, including complicated sample preparation, expensive professional instruments and well-trained individuals [1, 22]. More importantly, these techniques are unsuited for real-time monitoring and imaging of palladium in complicated biological samples, especially living cells, zebrafish and mice. To overcome this problem, variety of small molecule fluorescence probes are designed for detection of palladium. However, these reported fluorescent probes for palladium have several drawbacks, such as low fluorescence quantum yield, poor water solubility and long response time, which limited its applications (Table S1) [23-27]. As far as we know, few fluorescence probes have been reported for imaging palladium *in vivo*. Thus, development of a new water-soluble fluorescence probe for rapid detection and imaging of palladium *in vitro* and *in vivo* is of significance.

In this work, we present a novel colorimetric and fluorescent turn-on probe **NT-Pd**, (Scheme 1) for the sensitive and rapid response to palladium. **NT-Pd** was designed by the famous Tsuji-Trost reaction with naphthalimide group (**NT**) as the fluorophore and an allyl carbonate as the recognition group for palladium, as illustrated in Scheme 1 [28-29]. Naphthalimide was chosen as the excellent fluorophore due to its highly fluorescent quantum yield, good water-solubility and excellent biocompatibility, which may solve the problems described above [30-31]. As we expect, **NT-Pd** could successfully determine palladium in aqueous solution (10 mM PBS Buffer, pH=7.4). Under this condition of aqueous solution, **NT-Pd** displayed excellent sensing features, such as high selectivity and sensitivity in both colorimetric (colorless to yellow) and fluorescent (70-fold enhancement) methods, low detection limit (5.30 nM) and rapid response time (10 min). Most importantly, **NT-Pd** was successful applied for palladium imaging of living A549 cells and zebrafishes with extremely low toxicity, which confirmed **NT-Pd** has the potential capabilities for sensing of palladium *in vivo* and *in vitro*.



**Scheme 1.** Proposed mechanism of probe **NT-Pd** for detection of palladium.

## Materials and methods

**Reagents and Instruments.** All the reagents for the experiments were purchased from Sigma-Aldrich in analytical grade. The zebrafish and A549 cells were obtained from China Zebrafish Resource Center (Wuhan, China). The pH buffers were prepared through the METTLER TOLEDO Five Easy Plus pH meter. All the <sup>1</sup>H NMR and <sup>13</sup>C NMR spectra were recorded through a Varian 600 MHz spectrometer. The UV-vis spectra and fluorescence spectra were tested by SHIMADZU UV-1800 spectrophotometer and Agilent Cary Eclipse Fluorescence spectrophotometer respectively. The fluorescence imaging of living cells and zebrafishes was obtained with inverted fluorescence microscopy (Olympus IX71, Japan).

**Synthesis of probe.** The probe **NT-Pd** and fluorophore **NT** were synthesized as described in Scheme S1. In addition, the concrete synthesis route was displayed in Supplementary Information.

**Solution preparation and spectral measurement.** The probe **NT-Pd** (10 mM) was first dissolved in dimethyl sulfoxide. And the various testing analytes such as BaCl<sub>2</sub>, CaCl<sub>2</sub>, CuCl<sub>2</sub>, FeCl<sub>3</sub>, Hg(ClO)<sub>2</sub>, KCl, LiCl, MgSO<sub>4</sub>, MnCl<sub>2</sub>, NaCl, NiSO<sub>4</sub>, ZnCl<sub>2</sub>, Pd(PPh<sub>3</sub>)<sub>4</sub> were dissolved in ultrapure water (10 mM each). The different pH buffers (4.0, 5.0, 6.0, 7.0, 7.4, 8.0 and 9.0) were prepared for the detection of pH dependence. The fluorescence spectrum was tested at excitation wavelength was 450 nm.

**Calculation of the detection limit.** Based on our previous methods, the detection limit (DL) was calculated according to the following equation (1) [32-34]. The fluorescence spectrum of fluorescence probe and the standard deviation of blank measurement were measured. The linear relationship between fluorescence intensity of probe at 560 nm and concentration of Pd(PPh<sub>3</sub>)<sub>4</sub> was measured to get the slope.

$$DL = 3\sigma/k \quad (1)$$

Where  $\sigma$  and  $k$  are the standard deviation and the slope of the regression line, respectively.

**Determination of quantum yield.** According to the reported literature, the fluorescence quantum yields of **NT-Pd** and **NT** were tested by the following equation (2) [35-37]. The subscripts  $c$  and  $s$  represent the reference compound and sample respectively.  $\Phi_c$  is the quantum yield of fluorescein ( $\Phi=0.98$ , 0.1 M NaOH).  $F$  and  $A$  represented the fluorescence integral area and the absorbance, respectively.

$$\Phi_s = \frac{F_s \cdot A_c}{F_c \cdot A_s} \Phi_c \quad (2)$$

**Cell Cultures and Imaging.** A549 cells were cultured in Roswell Park Memorial Institute (RPMI-1640) supplemented with 10 % (v/v) FBS (fetal bovine serum), 1 % (v/v) penicillin/streptomycin on a cell culture flask in the atmosphere of 5 % CO<sub>2</sub> at 37 °C. The A549 cells were first seed in a plate for 24 h. Then, the probe (10 μM) was added into the cells for incubation 30 min at 37 °C. After washing the cells three times with PBS buffer to remove the residual probe, the A549 cells were further incubated with Pd(PPh<sub>3</sub>)<sub>4</sub> at different concentration (0, 25, 50 and 100 μM) for 30 min. All the cell imaging was acquired at green channel (510-550 nm).

**Imaging of Zebrafish.** Zebrafish embryos were purchased from China Zebrafish

Resource Center. The zebrafishes embryos were cultured in 200 mL medium containing 1-phenyl-2-thiourea (PTU) in a petrie dish for 48 h at 28 °C. After hatching zebrafish embryos, zebrafishes were first incubated with probe for 1 h at 28 °C. All the zebrafish samples were carefully washed to remove the residual probe. And the zebrafishes were further treated with different concentrations of Pd(PPh<sub>3</sub>)<sub>4</sub> (0, 25, 50, 100 μM) for another 2 h. At last, all the samples were imaged at green channel (510-550 nm).

## Results and Discussion

**Design and synthesis of probe NT-Pd.** In this work, **NT** was selected as the fluorophore due to its large Stokes' shift, long emission wavelength, high quantum yield, good water solubility and excellent biocompatibility. In addition, allylcarbonate moiety was considered to be a widely used recognition group in the design of palladium fluorescent probes. For instance, feng's group recently reported a selective and sensitive NIR fluorescent probe for palladium.[17] Based on this strategy, a novel fluorescence probe **NT-Pd** for palladium was designed through connect allylcarbonate moiety to **NT** via a well-known Tsuji-Trost reaction. Thus, **NT-Pd** was expected to be a sensitive and selective fluorescent probe for palladium. To verify this hypothesis, **NT-Pd** was synthesized following the detailed synthetic route depicted in Scheme S1. All the synthesized compounds were characterized by <sup>1</sup>H NMR, <sup>13</sup>C NMR and HR-MS, as shown in Figure S1-S9.

**Optical determination of NT-Pd to palladium.** In order to confirm the detection ability of probe **NT-Pd** to palladium, the absorbance spectra and fluorescence spectra had been measured in PBS buffer solution (10 mM, pH 7.4) at 30 °C. As we know, Pd(PPh<sub>3</sub>)<sub>4</sub> has been widely reported as the source of Pd<sup>0</sup>. Under this condition, as shown in Figure 1a, the absorption peak of **NT-Pd** (10 μM) at 450 nm has been apparent enhancement after treatment with 50 μM Pd<sup>0</sup>. And the color of the solution was obvious change from colorless to yellow under ambient light (insert of Figure 1a), confirming **NT-Pd** was an excellent probe for visual sensing of Pd<sup>0</sup>. Furthermore, as depicted in Figure 1b, the fluorescent spectra of **NT-Pd** was almost no fluorescence

with a low quantum yield ( $\Phi=0.005$ ), indicated that **NT-Pd** has extremely low fluorescence background. However, after being exposed to  $\text{Pd}^0$ , the fluorescence spectra of **NT-Pd** increased sharply in 10 min and without obvious change in the next 10 min. In addition, the insert picture depicted the fluorescence change from non-fluorescence to green fluorescence (insert of Figure 1b), which was in agreement with the test result. In order to measure the optimum reaction time, the fluorescence intensity of **NT-Pd** at 560 nm toward  $\text{Pd}^0$  was carried out (Figure S10). As depicted, the fluorescence intensity reached the approximate saturation at 10 min, and the fluorescence enhancement was calculated to be about 70-fold ( $\Phi=0.043$ ). It revealed that the best response time of **NT-Pd** for  $\text{Pd}^0$  was 10 min. All the experiment results clearly demonstrated that **NT-Pd** was a prospective probe for colorimetric and fluorescence response to  $\text{Pd}^0$ .

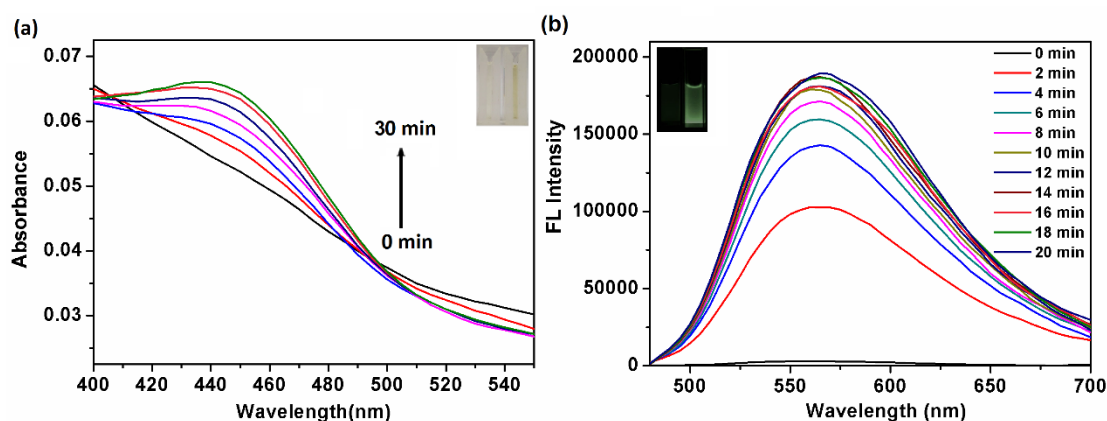


**Figure 1.** (a) Absorption spectra changes of probe **NT-Pd** ( $10 \mu\text{M}$ ) upon addition of  $\text{Pd}(\text{PPh}_3)_4$  ( $50 \mu\text{M}$ ) for different time. Inset: color changes. (b) Fluorescent spectra changes of **NT-Pd** ( $10 \mu\text{M}$ ) upon addition of  $\text{Pd}(\text{PPh}_3)_4$  ( $50 \mu\text{M}$ ).  $\lambda_{\text{ex}}=450 \text{ nm}$ . Inset (a, b): photographs of **NT-Pd** without or with  $\text{Pd}(\text{PPh}_3)_4$  under room light or UV light. All experiments were performed in PBS buffer ( $10 \text{ mM}$ ,  $\text{pH } 7.4$ ) at  $30 \text{ }^\circ\text{C}$ .

**Sensitivity of NT-Pd.** To further inspect the sensitivity of **NT-Pd**, the titration experiments of the **NT-Pd** sensing of different concentrations ( $0\text{-}300 \mu\text{M}$ ) of  $\text{Pd}^0$  were carried out in the assay. As displayed in Figure 2a, with the increase of concentration of  $\text{Pd}^0$ , the fluorescent intensity of **NT-Pd** at  $560 \text{ nm}$  was gradually increased. Moreover, the fluorescent intensity increased linearly at low concentration of  $\text{Pd}^0$  and reached saturation after incubation with  $200 \mu\text{M}$   $\text{Pd}^0$  (Figure 2b). This result indicated

that **NT-Pd** was a turn-on fluorescence probe for quantitative detection of  $\text{Pd}^0$ . Based on this, the detection limit of **NT-Pd** for  $\text{Pd}^0$  was further investigated. As revealed in Figure S11, a satisfactory linear relationship ( $Y=3646.32+10491.43[\text{Pd}^0]$ ,  $R^2=0.99501$ ) was established between the fluorescence intensity at 560 nm and concentrations of  $\text{Pd}^0$ . Hence, the detection limit (DL) was obtained as low as 5.38 nM by the method of equation  $DL=3\sigma/k$ , indicating **NT-Pd** was highly sensitive for sensing of  $\text{Pd}^0$ . Considering the rapid response to  $\text{Pd}^0$  (10 min) and low detection limit, it can be convinced that **NT-Pd** could sensitive detection of  $\text{Pd}^0$  at nanomolar level.

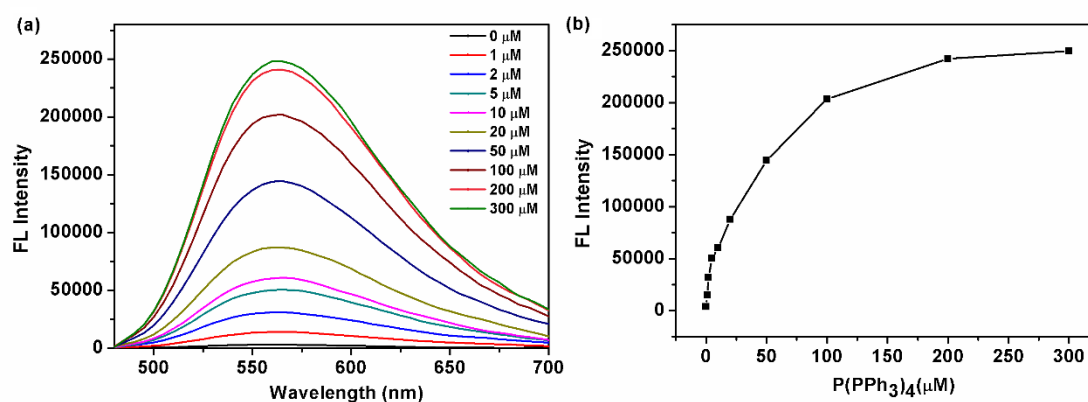


**Figure 2.** (a) Fluorescence change spectra of **NT-Pd** (10  $\mu\text{M}$ ) upon addition of increasing concentrations of  $\text{Pd}^0$  (0–300  $\mu\text{M}$ ) in PBS buffer (10 mM, pH 7.4) for 10 min at 30  $^{\circ}\text{C}$ . (b) Fluorescence intensity change of the **NT-Pd** at 560 nm as a function of the concentration of  $\text{Pd}^0$ .  $\lambda_{\text{ex}}=450$  nm.

**Reaction mechanism.** To understand the fluorescent turn-on mechanism of **NT-Pd** for sensing of  $\text{Pd}^0$ , the mixture system of **NT-Pd** and  $\text{Pd}^0$  was studied by HRMS. As illustrated in Figure S12a, the HRMS peak of pure probe **NT-Pd**  $[\text{M}+\text{Na}]^+$  (calcd. for 376.1160) was obvious observed. Besides, the mixture system of **NT-Pd** and  $\text{Pd}^0$  was also monitored through the HRMS. As depicted in Figure S12b, the extremely strong HRMS peak of fluorophore **NT**  $[\text{M}-\text{H}]^-$  (calcd. for 268.0974) was found, which illustrated **NT** was released through fracture allylcarbonate moiety of **NT-Pd**. Notably, these results clearly confirmed that the sensing mechanism **NT-Pd** for  $\text{Pd}^0$  was based on the Tsuji-Trost reaction, as we illustrated in Scheme 1.

**Theoretical Calculations.** In order to understand the quenching mechanism of

**NT-Pd**, we used Gaussian 09 program to calculate the frontier orbital energy of **NT** and **NT-Pd** at B3LYP/6-31G(d) level [38-39]. As shown in Figure 3, the highest occupied molecular orbital (HOMO) and lowest unoccupied molecular orbital (LUMO) of **NT** mainly located at naphthalimide rings and hydroxyl groups, while for **NT-Pd**, the orbitals showed a little delocalization compared with that of its fluorophore **NT**. Indicating that there was intramolecular charge transfer (ICT) effect between the fluorophore **NT** and allyl carbonate group of **NT-Pd**. The HOMO energy level of fluorophore **NT** was -6.10 eV, when allyl carbonate group was introduced the HOMO energy level of **NT-Pd** was decreased to -6.51 eV, suggested that the fluorescence of **NT** was quenched by the ICT process. Upon reacting with  $\text{Pd}^0$ , the non-fluorescence **NT-Pd** can release the fluorescent **NT**, our experimental results also confirmed the calculation results.

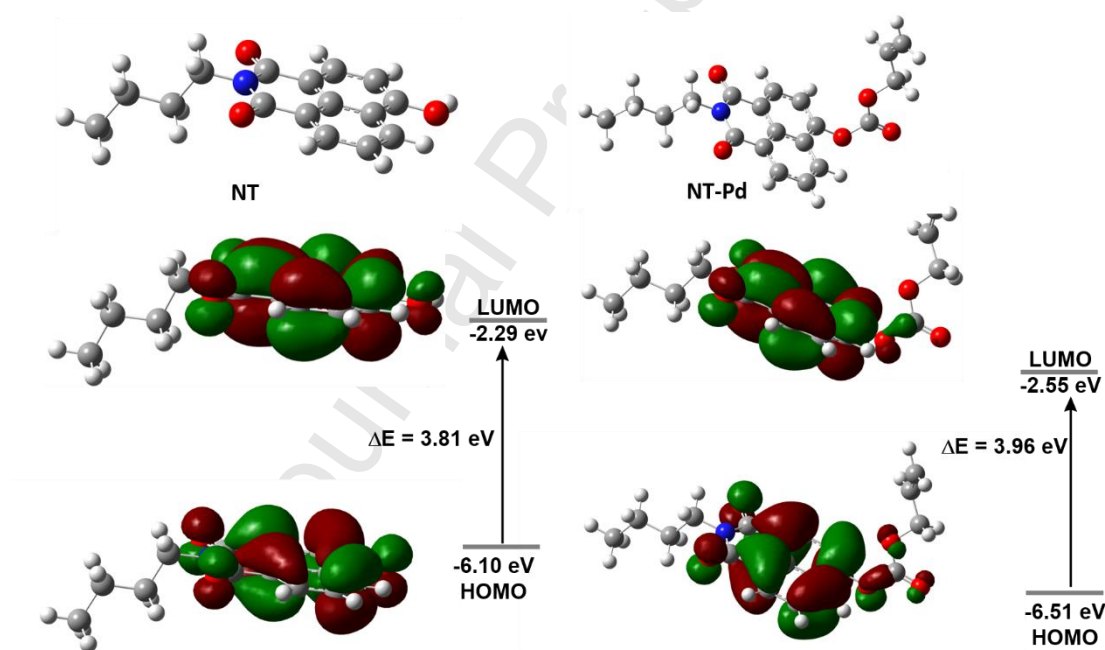


**Figure 3.** Optimized structures and frontier orbital energy of **NT** and **NT-Pd**. DFT calculations were performed by Gaussian 09 with B3LYP/6-31G(d) level.

**Selectivity of NT-Pd.** To evaluate the selectivity of **NT-Pd** for  $\text{Pd}^0$ , a number of interfering cations and anions, including  $\text{Ba}^{2+}$ ,  $\text{Ca}^{2+}$ ,  $\text{Cu}^{2+}$ ,  $\text{Fe}^{3+}$ ,  $\text{Hg}^{2+}$ ,  $\text{K}^+$ ,  $\text{Li}^+$ ,  $\text{Mg}^{2+}$ ,  $\text{Mn}^{2+}$ ,  $\text{Na}^+$ ,  $\text{Ni}^{2+}$ ,  $\text{Zn}^{2+}$ ,  $\text{CN}^-$ ,  $\text{ClO}^-$ ,  $\text{Br}^-$ ,  $\text{I}^-$  and  $\text{Pd}^{2+}$  were detected. As shown in Figure 4a, after adding various analytes (100  $\mu\text{M}$ ), the fluorescence signal of **NT-Pd** did not display significant changes. Compared to the interfering metal ions, the fluorescence

spectra of **NT-Pd** showed remarkably enhancement when added only 20  $\mu\text{M}$   $\text{Pd}^0$ . It indicated that **NT-Pd** exhibited highly selective for  $\text{Pd}^0$  against these cations (Figure 4b). Besides, **NT-Pd** also exhibited a specific selectivity against  $\text{Pd}^0$ , without any noticeable interference (Figure S13). Meanwhile, as a colorimetric probe **NT-Pd**, the selectivity of **NT-Pd** was also investigated in absorbance spectra. As depicted in Figure S14, the absorbance spectra of **NT-Pd** also showed high selectivity to  $\text{Pd}^0$ . In addition, this highly selectivity for  $\text{Pd}^0$  could be visibly seen by the naked eyes, because only  $\text{Pd}^0$  could change the color from colorless to yellow (insert of Figure S14). All of these experimental results confirmed that **NT-Pd** showed high selectivity and strongly anti-interference capability for sensing of  $\text{Pd}^0$  using both UV-vis and fluorescence method.

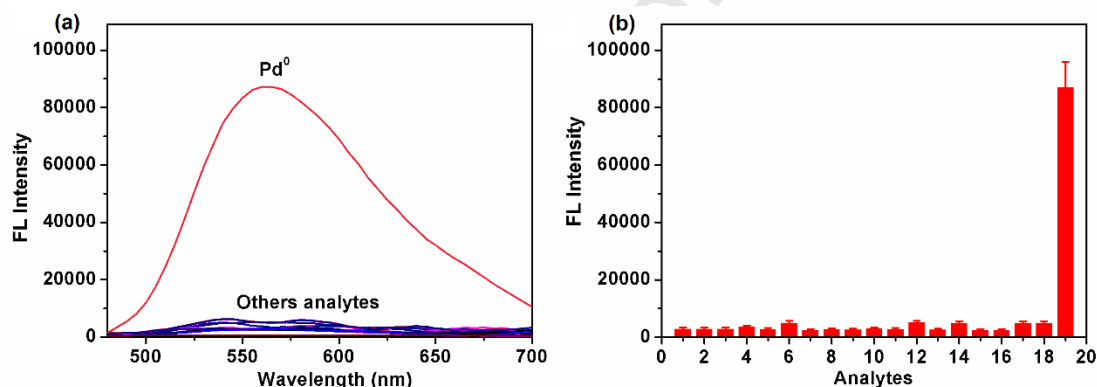


**Figure 4.** (a) Fluorescence spectra of **NT-Pd** for various analytes. (b) Fluorescence intensity responses of **NT-Pd** toward various analytes. (1. Blank, 2.  $\text{Ba}^{2+}$ , 3.  $\text{Ca}^{2+}$ , 4.  $\text{Cu}^{2+}$ , 5.  $\text{Fe}^{3+}$ , 6.  $\text{Hg}^{2+}$ , 7.  $\text{K}^+$ , 8.  $\text{Li}^+$ , 9.  $\text{Mg}^{2+}$ , 10.  $\text{Mn}^{2+}$ , 11.  $\text{Na}^+$ , 12.  $\text{Ni}^{2+}$ , 13.  $\text{Zn}^{2+}$ , 14.  $\text{CN}^-$ , 15.  $\text{ClO}^-$ , 16.  $\text{Br}^-$ , 17.  $\text{I}^-$ , 18.  $\text{Pd}^{2+}$ , 19.  $\text{Pd}^0$ .) The concentration of  $\text{Pd}^0$  was 20  $\mu\text{M}$ , and the other was 100  $\mu\text{M}$ . All experiments were monitor 10 min in PBS buffer (10 mM, pH 7.4) at 30  $^\circ\text{C}$ .  $\lambda_{\text{ex}}=450$  nm.

**pH effect.** The pH value of PBS buffer has affected the stability of **NT-Pd** and the response ability of **NT-Pd** for  $\text{Pd}^0$ , so the pH effect of **NT-Pd** for  $\text{Pd}^0$  was studied. As exposed in Figure S15, the fluorescent intensity of **NT-Pd** was almost unchanged over a wide pH rang (4-9), which verified its strong stability. However, when **NT-Pd** was treated with  $\text{Pd}^0$ , the fluorescent intensity increased sharply with the pH value from 4 to 7.4 and decreased gradually with the pH value from 7.4 to 9. Notably, the pH value at 7.4 was the optimal condition for sensing of  $\text{Pd}^0$ , indicating **NT-Pd** was suitable for detection  $\text{Pd}^0$  in living systems.

**Detection of Pd<sup>0</sup> in living cells.** To investigate the excellent sensing properties of probe **NT-Pd**, the bioimaging application of **NT-Pd** in A549 living cells was further explored. Prior to cell image, the cytotoxicity of **NT-Pd** at different concentrations (0, 1, 5, 10 and 20  $\mu\text{M}$ ) was assessed by using MTT assays in A549 cells for 18 h. As displayed in Figure S16, the highly cell viability of A549 cells clearly revealed that **NT-Pd** exhibited extremely low cytotoxicity. It illustrated **NT-Pd** could be applied for bioimaging in A549 cells. Consequently, the A549 cell imaging of **NT-Pd** for different concentrations of Pd<sup>0</sup> (0, 25, 50 and 100  $\mu\text{M}$ ) was investigated (Figure 5). The A549 cells showed almost no fluorescence when only incubated with **NT-Pd** for 30 min at 37 °C, indicating **NT-Pd** had low fluorescence background. Conversely, upon adding **NT-Pd** to the culture medium for another 30 min, the green fluorescence was obviously observed and gradually enhanced with the increased concentration of Pd<sup>0</sup>. It was also confirmed by the optical data, as depicted in Figure 5m. The cell cytotoxicity and imaging results revealed that **NT-Pd** could be permeate into cells and image Pd<sup>0</sup> with highly sensitivity.

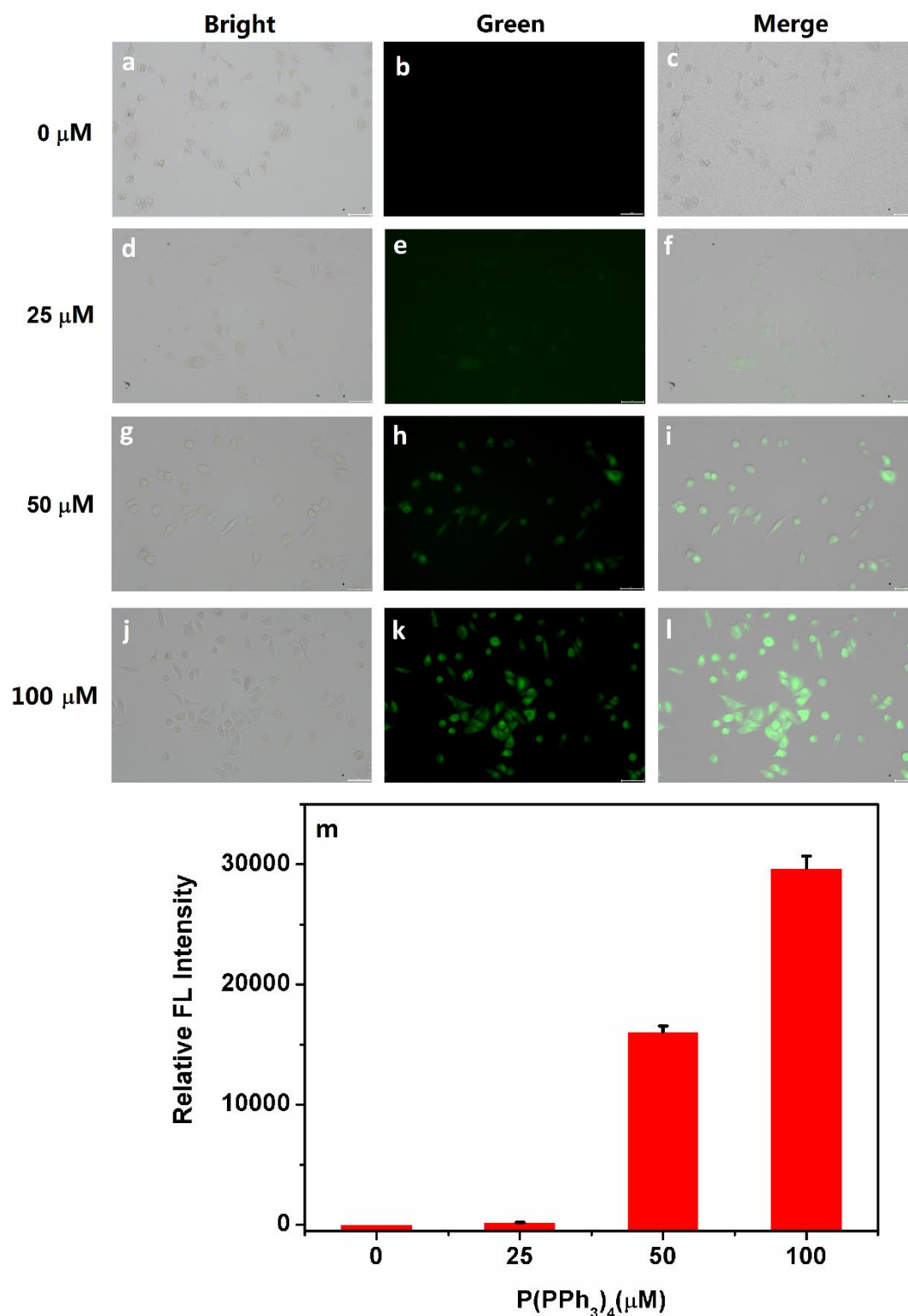


**Figure 5.** Fluorescence imaging of A549 cells for NT-Pd (10 μM) incubated with different concentrations of Pd<sup>0</sup> (0, 25, 50 and 100 μM). (a, d, g, j) bright field imaging, (b, e, h, k) green channel (550 - 580 nm), (c, f, i, l) merge imaging. (m) Relative fluorescence intensity of representative images with different concentrations of Pd<sup>0</sup> (0, 25, 50 and 100 μM). Data represent mean standard error (n=3), scale bar=40 μm.

**Zebrafish Imaging.** Zebrafish, one of the four classical model organisms, was widely applied for bioimaging [40-41]. Thus, due to the high selectivity and sensitivity of **NT-Pd** for  $\text{Pd}^0$ , the imaging ability of **NT-Pd** for zebrafish was further investigated, as depicted in Figure 6. One-week-old zebrafishes were incubated with **NT-Pd** for 0.5 h to ensure that the probe **NT-Pd** could be permeated into zebrafish, and following treatment with four groups of  $\text{Pd}^0$  (0, 25, 50 and 100  $\mu\text{M}$ ) for another 1 h. Each group of zebrafish was imaging by using a fluorescence microscope. As we expected, in absence of  $\text{Pd}^0$ , the zebrafish in the control group was undoubtedly alive and practically no fluorescent, indicating **NT-Pd** was an excellent probe for imaging in zebrafish with extremely low toxicity and fluorescence background. However, upon treating with  $\text{Pd}^0$ , the fluorescence of the zebrafish was clearly observed, and gradually enhanced with the increase concentrations of  $\text{Pd}^0$ . As depicted in Figure 6m, the relative fluorescence intensity of zebrafish revealed that **NT-Pd** could detect exogenous  $\text{Pd}^0$  by fluorescent imaging. All of these resulted demonstrated that probe **NT-Pd** was able to image of  $\text{Pd}^0$  in living body with good biocompatibility and high sensitivity.

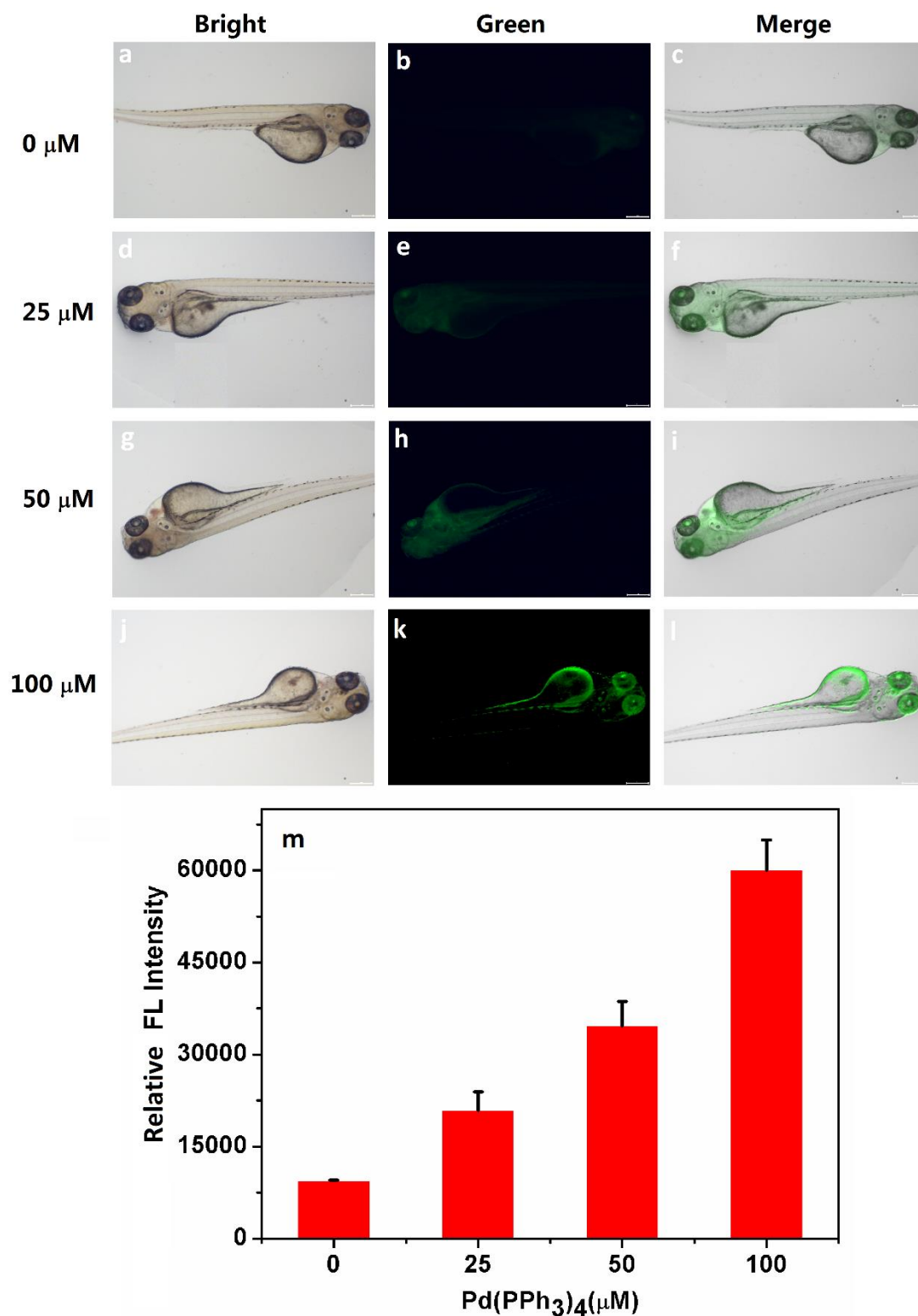


**Figure 6.** Fluorescence imaging of zebrafish for **NT-Pd** (10  $\mu\text{M}$ ) incubated with different concentrations of  $\text{Pd}^0$  (0, 25, 50 and 100  $\mu\text{M}$ ) for 30 min. (a, d, g, j) bright field imaging, (b, e, h, k) green channel (550 - 580 nm), (c, f, i, l) merge imaging. (m) Relative fluorescence intensity of representative images with different concentrations of  $\text{Pd}^0$  (0, 25, 50 and 100  $\mu\text{M}$ ). Data represent mean standard error (n=3), scale bar=200  $\mu\text{m}$ .

## Conclusion

In summary, a novel probe **NT-Pd** was designed for colorimetric and fluorescent turn-on detection of palladium *in vitro* and *in vivo*. This new probe had excellent selectivity and sensitivity to palladium in phosphate buffer at physiological pH, which exhibited a rapid fluorescent turn-on response (10 min) and distinct color change. Furthermore, the **NT-Pd** could be used for the quantitative determination of palladium with a detection limit of 5.30 nM. In addition, **NT-Pd** has good biocompatibility and low toxicity, which could contribute to its successful use in tracking palladium in living cells and zebrafish model. Overall, all these features illustrated that **NT-Pd** was a very promising tool for sensing of palladium in complicated biological system.

## Acknowledgment

This work was financially supported by the National Natural Science Foundation of China (21804102), the Outstanding Young and Middle-aged Scientific Innovation Team of Colleges and Universities of Hubei Province: "Biomass chemical technologies and materials" (Grant No. T201908), the National Key R&D Program of China (2017YFE0118200), the Anhui Key Research and Development Program (No. 201904b11020025), the Anhui Natural Science Fund Project (No. 1908085MB35) and the Natural Science Research Project of Anhui Higher Education Institution (Key Project, No. KJ2018A0040).

## References

- [1] B. Ke, H. Chen, Y. Cui, L. Ma, Y. Liu, X. Hu, Y. Bai, L. Du, M. Li, A bioluminescent strategy for imaging palladium in living cells and animals with chemoselective probes based on luciferin-luciferase system, *Talanta* 194 (2018) 925-929.
- [2] C. Locatelli, D. Melucci, G. Torsi, Determination of platinum-group metals and lead in vegetable environmental bio-monitors by voltammetric and spectroscopic techniques: critical comparison, *Anal. Bioanal. Chem.* 382 (2005) 1567-1573.

- [3] T. Schwarze, H. Müller, C. Dosche, T. Klamroth, W. Mickler, A. Kelling, H. G. Löhmansröben, P. Saalfrank, H. J. Holdt, Luminescence detection of open-shell transition-metal ions by photoinduced electron transfer controlled by internal charge transfer of a receptor, *Angew. Chem. Int. Ed.* 46 (2007) 1671-1674.
- [4] H. Cui, H. Chen, Y. Pan, W. Lin, A two-photon fluorescent turn-on probe for palladium imaging in living tissues, *Sens. Actuators B Chem.* 219 (2015) 232-237.
- [5] T. Chen, C. Q. Zhao, L. B. Han, Hydrophosphorylation of alkynes catalyzed by palladium: generality and mechanism, *J. Am. Chem. Soc.* 140 (2018) 3139-3155.
- [6] S. Ma, B. Wu, X. Jiang, PdCl<sub>2</sub>-catalyzed efficient transformation of propargylic amines to (*E*)- $\alpha$ -chloroalkylidene- $\beta$ -lactams, *J. Org. Chem.* 70 (2005) 2588-2593.
- [7] C. Sui, G. Lu, X. Y. Li, Z. P. Qu, X. J. Zou, G. H. Chen, Selective oxidation of cyclopentene catalyzed by Pd(CH<sub>3</sub>COO)<sub>2</sub>-NPMoV under oxygen atmosphere, *React. Kinet. Catal. L.* 94 (2008) 191-198.
- [8] S. Ganesamoorthy, K. Shanmugasundaram, R. Karvembu, Remarkable catalytic activity of [PdCl<sub>2</sub>(CH<sub>3</sub>CN)<sub>2</sub>] in Suzuki–Miyaura cross-coupling reaction in aqueous media under mild conditions, *J. Mol. Catal. A-Chem.* 371 (2013) 118-124.
- [9] M. Y. Alfaifi, S. E. I. Elbehairi, H. S. Hafez, R. F. M. Elshaarawy, Spectroscopic exploration of binding of new imidazolium-based palladium(II) sandwich complexes with CT-DNA as anticancer agents against HER2/neu overexpression, *J. Mol. Struct.* 1191 (2019) 118-128.
- [10] Z. Sorinezami, H. Mansouri-Torshizi, M. Aminzadeh, A. Ghahghaei, N. Jamgohari, M. Heidari Majd, Synthesis of new ultrasonic-assisted palladium oxide nanoparticles: an in vitro evaluation on cytotoxicity and DNA/BSA binding properties. *J. Biomol. Struct. Dyn.* 37 (2019) 4238-4250.
- [11] X. Chen, H. Li, L. Jin, B. Yin, A ratiometric fluorescent probe for palladium detection based on an allyl carbonate group functionalized hemicyanine dye, *Tetrahedron Lett.* 55 (2014) 2537-2540.

- [12] J. Qin, X. Li, Z. Chen, F. Feng, A highly selective and commercially available fluorescence probe for palladium detection, *Sens. Actuators B Chem.* 232 (2016) 611-618.
- [13] C. L. S. Wiseman, F. Zereini, Airborne particulate matter, platinum group elements and human health: A review of recent evidence, *Sci. Total Environ.* 407 (2009) 2493-2500.
- [14] C. D. Spicer, T. Triemer, B. G. Davis, Palladium-mediated cell-surface labeling, *J. Am. Chem. Soc.* 134 (2012) 800-803.
- [15] R. M. Yusop, A. Unciti-Broceta, E. M. V. Johansson, R. M. Sánchez-Martín, M. Bradley, Palladium-mediated intracellular chemistry, *Nat. Chem.* 3 (2011) 239-243.
- [16] C. Garrett, K. Prasad, The art of meeting palladium specifications in active pharmaceutical ingredients produced by Pd-catalyzed reactions, *Adv. Synth. Catal.* 346 (2004) 889-900.
- [17] Q. Xia, S. Feng, D. Liu, G. Feng, A highly selective and sensitive colorimetric and near-infrared fluorescent turn-on probe for rapid detection of palladium in drugs and living cells, *Sens. Actuators B Chem.* 258 (2018) 98-104.
- [18] A. V. Volzhenin, N. I. Petrova, N. S. Medvedev, D. S. Irisov, A. I. Saprykin, Determination of gold and palladium in rocks and ores by atomic absorption spectrometry using two-stage probe atomization, *J. Anal. Chem.* 72 (2017) 156-162.
- [19] O. Borisov, D. Coleman, K. Oudsema, R. Carter, Determination of platinum, palladium, rhodium and titanium in automotive catalytic converters using inductively coupled plasma mass spectrometry with liquid nebulization, *J. Anal. At. Spectrom.* 12 (1997) 239-246.
- [20] Y. J. Dong, Liquid-liquid microextraction coupled with high performance liquid chromatography for determination of palladium, *J. Chin. Chem. Soc.* 55 (2008) 567-571.
- [21] M.K. Van, A. Smekens, M. Behets, P. Kazandjian, G.R. Van, Determination of platinum, palladium, and rhodium in automotive catalysts using

- high-energy secondary target X-ray fluorescence spectrometry, *Anal. Chem.* 79 (2007) 6383-6389.
- [22] X. Teng, M. Tian, J. Zhang, L. Tang, J. Xin, A TCF-based colorimetric and fluorescent probe for palladium detection in an aqueous solution, *Tetrahedron Lett.* 59 (2018) 2804-2808.
- [23] J. W. Yan, X. L. Wang, L. F. Zhou, L. Zhang, CV-APC, a colorimetric and red-emitting fluorescent dual probe for the highly sensitive detection of palladium, *RSC Adv.* 7 (2017) 20369-20372.
- [24] J. Jiang, H. Jiang, W. Liu, X. Tang, Xi Zhou, W. Liu, R. Liu, A colorimetric and ratiometric fluorescent probe for Palladium, *Org. Lett.* 13 (2011) 4922-4925.
- [25] W. Su, B. Gu, X. J. Hu, X. L. Duan, Y. Y. Zhang, H. T. Li, S. Z. Yao, A near-infrared and colorimetric fluorescent probe for palladium detection and bioimaging, *Dyes Pigm.* 137 (2017) 293-298.
- [26] W. Luo, W. Liu, A two-photon ratiometric ESIPT probe for discrimination of different palladium species and its application in bioimaging, *J. Mater. Chem. B* 4 (2016) 3911-3915.
- [27] H. Li, J. Fan, J. Du, K. Guo, S. Sun, X. Liu, X. Peng, A fluorescent and colorimetric probe specific for palladium detection, *Chem. Commun.* 46 (2010) 1079-1081.
- [28] M.P. Tracey, D. Pham, K. Koide, Fluorometric imaging methods for palladium and platinum and the use of palladium for imaging biomolecules, *Chem. Soc. Rev.* 44 (2015) 4769-4791.
- [29] H. Li, J. Fan, X. Peng, Colourimetric and fluorescent probes for the optical detection of palladium ions, *Chem. Soc. Rev.* 42 (2013) 7943-7962.
- [30] Z. Xu, J. Yoon, D. R. Spring, A selective and ratiometric Cu<sup>2+</sup> fluorescent probe based on naphthalimide excimer-monomer switching, *Chem. Commun.* 46 (2010) 2563-2565.
- [31] A. P. D. Silva, H. Q. N. Gunaratne, J. L. Habib-Jiwan, C. P. McCoy, T. E. Rice, J. P. Soumillion, New fluorescent model compounds for the study of photoinduced electron transfer: the influence of a molecular electric field in the excited state, *Angew. Chem. Int. Ed.* 34 (1995) 1728-1731.
- [32] H. Xu, M. Hepel, "Molecular beacon"-based fluorescent assay for selective detection of glutathione and cysteine, *Anal. Chem.* 83 (2011) 813-819.

- [33] Y. Zhou, J. Yan, N. Zhang, D. Li, S. Xiao, K. Zheng, A ratiometric fluorescent probe for formaldehyde in aqueous solution, serum and air using aza-cope reaction, *Sens. Actuators B Chem.* 258 (2017) 156-162.
- [34] T. Wang, Y. Chai, S. Chen, G. Yang, C. Lu, J. Nie, C. Ma, Z. Chen, Q. Sun, Y. Zhang, J. Ren, F. Wang, W. H. Zhu, Near-infrared fluorescent probe for imaging nitroxyl in living cells and zebrafish model, *Dyes Pigm.* 166 (2019) 260-265.
- [35] J. Li, Y. Cui, C. Bi, S. Feng, F. Yu, E. Yuan, S. Xu, Z. Hu, Q. Sun, D. Wei, J. Yoon, Oligo (ethylene glycol)-functionalized ratiometric fluorescent probe for the detection of hydrazine in vitro and vivo, *Anal. Chem.* 91 (2019) 7360-7365.
- [36] S. Yuan, F. Wang, G. Yang, C. Lu, J. Nie, Z. Chen, J. Ren, Y. Qiu, Q. Sun, C. Zhao, W. H. Zhu, A highly sensitive ratiometric self-assembled micellar nanoprobe for nitroxyl and its application in vivo, *Anal. Chem.* 90 (2018) 3914-3919.
- [37] Z. Zhou, F. Wang, G. Yang, C. Lu, J. Nie, Z. Chen, J. Ren, Q. Sun, C. Zhao, W. H. Zhu, A ratiometric fluorescent probe for monitoring Leucine aminopeptidase in living cells and zebrafish model, *Anal. Chem.* 89 (2017) 11576-11582.
- [38] R. Ren, H. C. Xu, H. Dong, H. T. Peng, P. P. Wu, Y. Qiu, S. G. Yang, Q. Sun, N. F. She, Ultrafast 2,7-naphthyridine-based fluorescent probe for detection of thiophenol with a remarkable Stokes shift and its application in vitro and in vivo, *Talanta* 205 (2019) 12067.
- [39] H. Lv, G. Yuan, G. Zhang, Z. Ren, H. He, Q. Sun, X. Zhang, S. Wang, A novel benzopyran-based colorimetric and near-infrared fluorescent sensor for  $Hg^{2+}$  and its imaging in living cell and zebrafish, *Dyes Pigm.* 172 (2020) 107658.
- [40] S. Hu, T. Wang, J. Zou, Z. Zhou, C. Lu, J. Nie, C. Ma, G. Yang, Z. Chen, Y. Zhang, Q. Sun, Q. Fei, J. Ren, F. Wang, Highly chemoselective fluorescent probe for the detection of tyrosinase in living cells and zebrafish model, *Sens. Actuators B Chem.* 283 (2019) 873-880.
- [41] X. Zhang, H. Liu, Y. Ma, W. Qu, H. He, X. Zhang, S. Wang, Q. Sun, F. Yu, Development of a novel near-infrared fluorescence light-up probe with a large

Stokes shift for sensing of cysteine in aqueous solution, living cells and zebrafish.

Dyes Pigm. 171 (2019) 107722.

Journal Pre-proof

**Credit Author Statement**

There is no conflict of interest between the authors and they abide by the academic ethics.

Journal Pre-proof

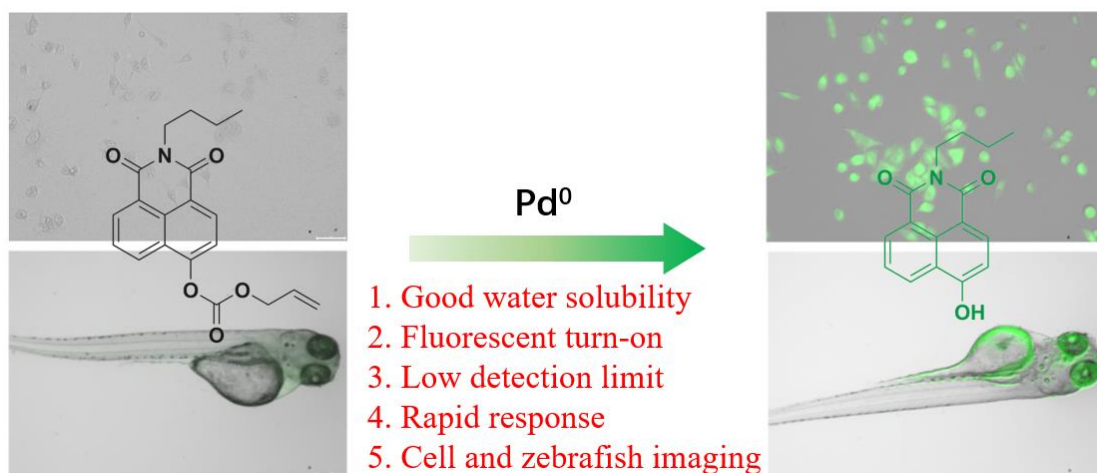
**Declaration of interests**

The authors declare that they have no known competing financial interests or personal relationships that could have appeared to influence the work reported in this paper.

The authors declare the following financial interests/personal relationships which may be considered as potential competing interests:

Journal Pre-proof

## Graphical Abstract



## Highlights

- A novel colorimetric and fluorescent probe **NT-Pd** was constructed for detection of palladium.
- The probe **NT-Pd** was able to detect palladium in aqueous solution.
- The probe **NT-Pd** exhibited high selectivity and sensitivity to palladium.
- The probe **NT-Pd** could be used for imaging of palladium in living A549 cells and zebrafishes.

Journal Pre-proof